nature chemistry

ARTICLES

PUBLISHED ONLINE: 1 AUGUST 2010 | DOI: 10.1038/NCHEM.765

Organic structure determination using atomic-resolution scanning probe microscopy

Leo Gross[1]*, Fabian Mohn[1], Nikolaj Moll[1], Gerhard Meyer[1], Rainer Ebel[2], Wael M. Abdel-Mageed[2,3] and Marcel Jaspars[2]

Nature offers a huge and only partially explored variety of small molecules with potential pharmaceutical applications. Commonly used characterization methods for natural products include spectroscopic techniques such as nuclear magnetic resonance spectroscopy and mass spectrometry. In some cases, however, these techniques do not succeed in the unambiguous determination of the chemical structure of unknown compounds. To validate the usefulness of scanning probe microscopy as an adjunct to the other tools available for organic structure analysis, we used the natural product cephalandole A, which had previously been misassigned, and later corrected. Our results, corroborated by density functional theory, demonstrate that direct imaging of an organic compound with atomic-resolution force microscopy facilitates the accurate determination of its chemical structure. We anticipate that our method may be developed further towards molecular imaging with chemical sensitivity, and will become generally useful in solving certain classes of natural product structures.

Scanning probe microscopy (SPM) has become an important tool for the study of biologically relevant molecules, and scanning tunnelling microscopy (STM) has been used to study DNA molecules for more than 25 years[1–5]. Indeed, the partial sequencing of a single DNA molecule with STM has recently been demonstrated[6]. Atomic force microscopy (AFM) has been successfully used to achieve near-atomic resolution on microfibrils[7] and proteins[8]. Achieving atomic resolution on organic compounds, however, remains a great challenge. Only recently has an entire molecule been resolved atomically by means of non-contact AFM[9]. In this study we attempt to tackle the question of whether this technique can be used to determine the atomic structure of unknown molecules.

Although a number of well-established methods are available, the *ab initio* structural characterization of natural products can be very challenging. This is particularly the case when using nuclear magnetic resonance (NMR) methods on systems for which there are a limited number of protons, where the carbon skeleton is interrupted by heteroatoms, or where there are quaternary carbons that have no long-range correlations to protons[10]. All these features are often present in the planar molecules isolated from a range of marine invertebrates and microorganisms[11,12], and it is often the case that an X-ray crystallographic solution is not possible owing to a lack of suitable crystals. In many situations, the resulting structure cannot then be confirmed without a complex and lengthy synthesis process[13,14]. A comprehensive literature search (1975–2009) of natural products of marine origin for which the structures have been corrected showed that of approximately 280 structures, 17% are planar and a further 13% have planar moieties that are amenable to the approach we report here, potentially leading to a great saving in synthetic effort (Crews, P. *et al.*, personal communication, 2010). We demonstrate the first successful use of non-contact AFM with atomic resolution to assist in the determination of the molecular connectivity of a natural product that had previously been misassigned.

Results

Nuclear magnetic resonance. In our search for novel natural products with potential pharmaceutical applications, we were fortunate to work on the pressure-tolerant actinobacterium *Dermacoccus abyssi*, which was isolated from a sediment collected from the deepest place on Earth, Challenger Deep in the Mariana Trench[15]. Several compounds of interest were extracted from this bacterium, among them the metabolite that is the subject of this report. The chemical formula of the metabolite under investigation was quickly determined to be $C_{16}H_{10}N_2O_2$ by high-resolution mass spectrometry (MS), indicating that there were 13 degrees of unsaturation in the structure.

Structure elucidation of unknowns using state-of-the-art NMR spectroscopy relies heavily on two-dimensional experiments, including correlation spectroscopy (COSY) and heteronuclear multiple bond correlation (HMBC), which detect interactions (couplings) of neighbouring protons (2–4 bonds) with each other or with neighbouring carbon atoms (2–3 bonds), respectively[10]. We obtained one- and two-dimensional NMR data sets in different solvents, and the very sparse COSY data set showed two spin systems, H5–H6–H7–H8 and H4′–H5′–H6′–H7′ (Fig. 1; details about the spectroscopic analysis can be found in the Supplementary Information). The quaternary carbons C4a and C8a were placed using HMBC correlations from C8a to H7 and H8 and from C4a to H6. It was clear that this was an isolated substructure and that the carbon skeleton was interrupted at both these points by quaternary carbons and/or heteroatoms. The second spin system H4′–H5′–H6′–H7′ was extended by the placement of the two quaternary carbons C3a′ and C7a′ using HMBC correlations to H5′ and H6′, respectively. Further extension to an indole moiety was possible using HMBC correlations C3a′ and C7a′ to H2′ and C3′ to H4′. An additional quaternary carbon, C3, was connected to one of the indole pyrrole ring carbons through the use of the HMBC correlation C3 to H2′.

At this point, a complete set of substructures could be assembled, which included the two alternative substitution patterns for the

[1]IBM Research — Zurich, 8803 Rüschlikon, Switzerland, [2]Marine Biodiscovery Centre, Department of Chemistry, University of Aberdeen, AB24 3UE, UK, [3]Department of Pharmacognosy, Faculty of Pharmacy, Assiut University, Assiut, Egypt. *e-mail: LGR@zurich.ibm.com

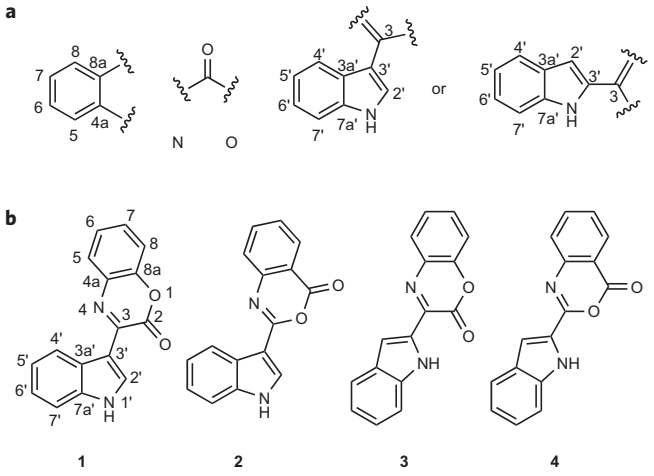

Figure 1 | Structures derived from NMR data. a, Three substructures could be identified from the two-dimensional NMR data sets. High-resolution mass spectrometry data indicate the presence of further N and O atoms in the structure. The available NMR data did not allow distinction between a two or three substituted indole substructure. **b**, The substructures can be combined into four possible compounds (**1** to **4**) consistent with the available data. **1** is the accepted structure of cephalandole A, and **2** is the previously misassigned structure of this compound.

indole substructure that are commonly found (Fig. 1a). These substructures could be assembled into the four possible working structures **1** to **4** shown in Fig. 1b. Structure **1** (which we were later able to determine as being the correct structure of our unknown metabolite, as will be shown below) is known as cephalandole A and was originally isolated from the Taiwanese orchid *Cephalanceropsis gracilis* (Orchidaceae)[16,17]. It meets all three criteria specified previously that render structure analysis especially challenging[10]: in **1**, the ratio of heavy atoms to protons is 2:1, and the O and N atoms at positions 1 and 4, respectively, interrupt the carbon skeleton completely, thus separating the two parts of the molecule. Furthermore, the carbonyl at C2 is four bonds removed from the nearest proton and is not expected to show correlations in an HMBC experiment. In fact, because of these difficulties, cephalandole A was initially misassigned as structure **2** in the original investigation[16], and later corrected[17], which makes it an excellent candidate for demonstrating the capabilities of our new approach. For us, at this point, all four working structures in Fig. 1b were plausible, as there were no HMBC correlations to guide us in the assembly of the substructures and each bicycle proposed in these structures had been reported previously[17].

Scanning probe microscopy. To resolve and confirm the molecular structure, we then conducted STM and AFM measurements on individual specimens of the compound in question. To this end, we deposited a low coverage of the molecules onto two-monolayer (ML) thick NaCl films grown on Cu(111). Our measurements were performed with a combined low-temperature STM/AFM based on a qPlus tuning fork sensor design[18]. The AFM was operated in the frequency modulation mode[19] and at very small oscillation amplitudes to maximize the lateral resolution[20]. We functionalized the tip apex of the microscope by controlled pickup of a single CO molecule, which was recently shown to dramatically increase AFM resolution on molecules[9]. The STM image of the metabolite (Fig. 2a) shows submolecular resolution, vaguely reminiscent of molecular images obtained by scanning tunnelling hydrogen microscopy (STHM)[21,22] (Supplementary Fig. S1). In the AFM image (Fig. 2b) it was possible to partly observe the molecular structure, with indications of atom sites, intermolecular bonds and cyclic systems.

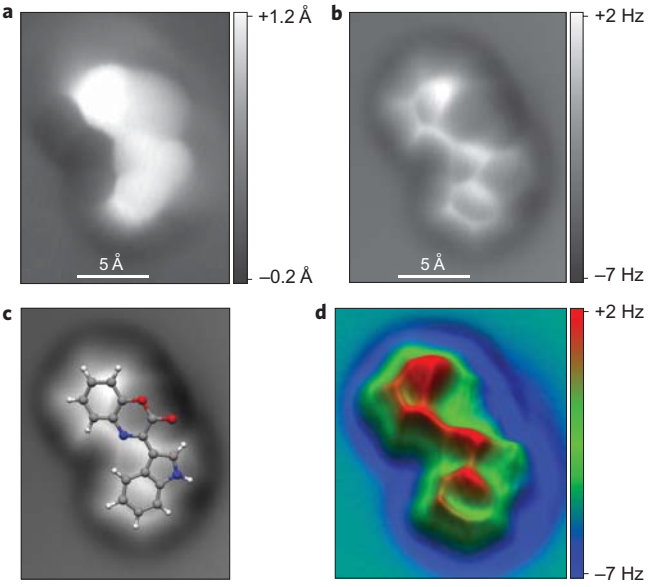

Figure 2 | SPM measurements of the unknown compound. STM and AFM measurements with a CO-functionalized tip were performed on a specimen adsorbed on the NaCl(2 ML)/Cu(111) surface. Image size: 16 Å × 19 Å. **a**, Constant-current STM measurement (tunnelling current $I = 1.2$ pA, sample voltage $V = 150$ mV). **b**–**d**, Constant-height AFM measurement (oscillation amplitude $A = 0.5$ Å, sample voltage $V = 0$ mV). The images show the original raw data (**b**), the same image with the molecular model of cephalandole A (**1**) overlaid as a guide to the eye (**c**) and a low-pass filtered three-dimensional representation (**d**). By direct comparison with the structures shown in Fig. 1, structures **3** and **4** can be ruled out.

From previous investigations it is known that the dark halo surrounding the molecules arises mainly due to van der Waals and electrostatic interactions between the tip and the molecule, whereas the atomic corrugation is mainly due to Pauli repulsive forces leading to the bright (repulsive) features, reflecting atom sites and intramolecular bonds[9]. Therefore, AFM images can be directly compared with the molecular models, and we tried to match the four molecular models determined from the spectroscopic data with the AFM images. Upon assessing the latter, the placement of the indole bicycle was immediately clear, namely, on the lower right-hand side of the images shown in Fig. 2, where a six-membered ring connected to a five-membered ring is visible. Structures **3** and **4** could now already be ruled out, because the angle between the two bicyclic systems cannot be brought into accordance with the AFM measurements. This left only cephalandole A (**1**) and the previously misassigned structure **2** as candidates. In Fig. 2c, the model of **1** has been overlaid on the AFM image. However, not all the details in the AFM image could be explained and the molecular structure is not resolved clearly in all parts of the molecule. Structure **2** could not be excluded at this stage, because we did not obtain atomic contrast at the positions of C2 and the neighbouring oxygen atoms, which distinguish structure **1** from **2**. Note that in contrast to the previously studied planar hydrocarbon pentacene[9], the bacterial metabolite has the following features: (i) it is not planar, mainly because of possible torsion about the central C–C bond connecting the two bicyclic systems; (ii) it consists of several atomic species including oxygen and nitrogen, possibly with different coordination numbers; and (iii) it exhibits no symmetry planes. The limited contrast in the region close to the oxygen atoms might therefore reflect chemical sensitivity, that is, different interactions due to the atomic species[23], or might be caused by topographic effects; that is, it might be due to non-planar adsorption of the molecule.

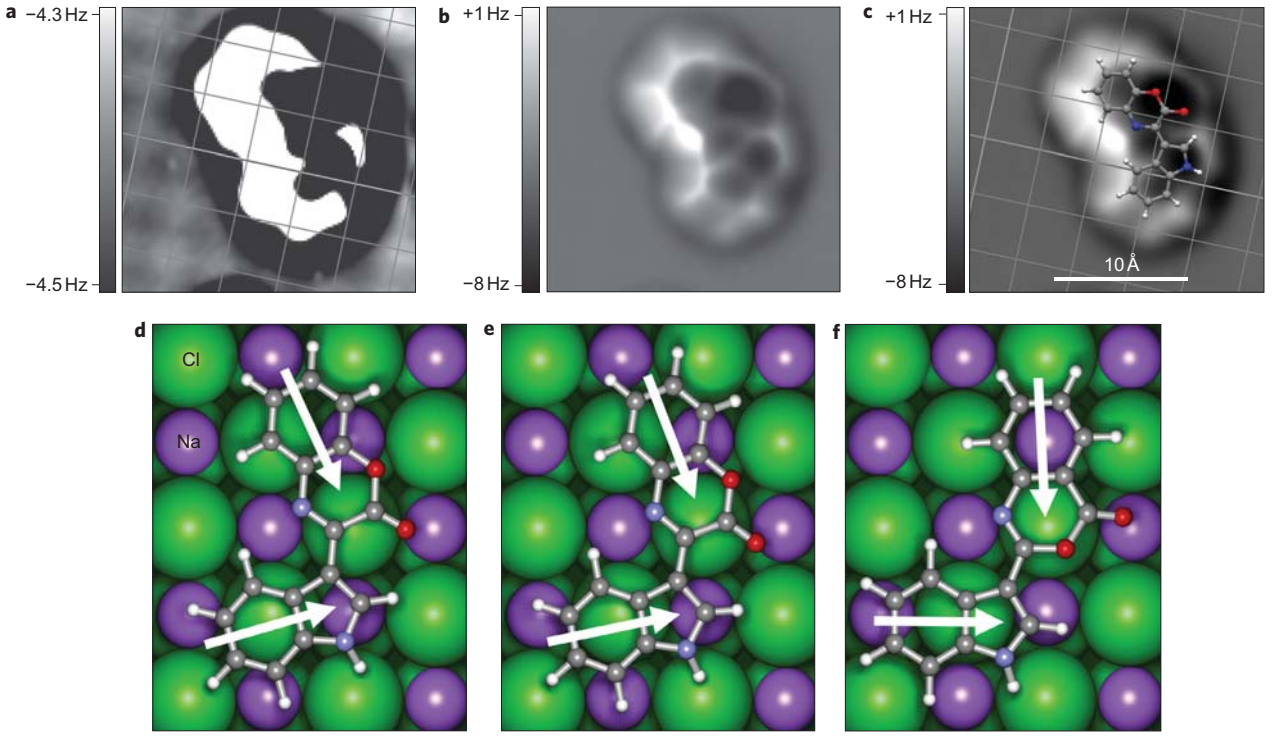

Figure 3 | Determination of the adsorption position. a–c, AFM with STM feedback; that is, the Δf channel recorded with constant-current feedback. Images **a–c** show the same data, but with different Δf scales (imaging parameters: $V = 150$ mV, $I = 1.2$ pA, $A = 0.5$ Å; image size 21 Å × 21 Å). With a Δf scale of 0.2 Hz (**a**) the substrate atomic positions can be deduced and a grid indicating the Cl positions is overlaid. With a Δf scale of 9 Hz (**b**) atomic contrast above the molecule is observed and the molecular position and orientation can be extracted. Panel **c** presents the same image as in **b**, but with the Cl grid of **a** and model of structure **1** overlaid. **d**, Molecular adsorption position as determined from experimental data. **e**,**f**, DFT-calculated adsorption geometries for **1** and **2**, respectively. White arrows indicating the orientation of the bicyclic systems have been added as a guide to the eye. The agreement between **d** and **e** and the disagreement between **d** and **f** allow structural assignment as **1**.

All molecules observed on the surface (more than 100) showed similar contrast in STM measurements (as shown in Fig. 2a) or with mirrored symmetry. The latter case we attribute to adsorption with the opposite side of the molecule facing the substrate. Furthermore, the high-resolution AFM measurements using CO-modified tips, conducted on about ten different molecules, always showed similar or mirrored contrast, as shown in Fig. 2b, indicating that only one molecular species was evaporated onto the sample.

As a next step, we determined the adsorption position of the molecule on NaCl. We used the STM constant-current feedback to control the tip height, while at the same time oscillating the tip and recording the shift Δf of the oscillation frequency, that is, the AFM signal. Figure 3a–c shows the AFM signal that has been recorded simultaneously with the STM topography shown in Fig. 2a. In this measurement mode, the STM and AFM signals are convoluted, which makes quantitative interpretation difficult. However, this mode allowed us to atomically resolve the substrate and the molecule at the same time, in contrast to the constant-height AFM measurements shown above. In comparison with the STM measurements (Supplementary Fig. S1), we assigned the faint maxima in Fig. 3a to the Cl sites of the NaCl substrate. The atomic grid determined was used as a reference to identify the molecular adsorption position, as shown in Fig. 3c, where the grid crossings indicate the Cl positions of the substrate. A determination of the adsorption position using only STM data yielded an identical position and orientation within measurement accuracy (Supplementary Fig. S1). We estimate errors of ∼0.5 Å for the adsorption site and $\sim\pm5^\circ$ for the in-plane orientation. In Fig. 3d, a model of the experimentally determined adsorption position for **1** is displayed. Note that the assumption of **2** would have led to an identical adsorption position, because the positions of C2 and the oxygen atoms were not taken into account in matching the model with the AFM image.

Density functional theory. To distinguish **1** from **2**, we carried out density functional theory (DFT) calculations[24,25] for comparison with the experimentally determined adsorption site. As a starting condition, we placed the molecule onto the NaCl surface close to the experimentally determined adsorption position. From this starting condition, all the atoms in the system, except the two bottom NaCl layers, were relaxed, yielding the adsorption positions shown in Fig. 3e and f for **1** and **2**, respectively. Comparison with the experimentally determined adsorption position (Fig. 3d) yields a good agreement in terms of adsorption position and orientation for **1** (Fig. 3e), but a significant mismatch for **2** (Fig. 3f). For example, the discrepancy of the in-plane orientation of the indole group is 4° for **1** and 16° for **2**. Therefore, we can conclusively rule out **2** as a last possible alternative structure of the molecule under investigation.

Using the calculated adsorption geometry of the molecule shown in Fig. 3e, we simulated an AFM image of **1** with DFT. The tip was modelled only by a CO molecule with the oxygen atom pointing towards the surface plane, which was previously proven to be a reasonable assumption[9]. The frequency shift was calculated as the second derivative of the interaction energy with respect to the intermolecular distance d. A calculated Δf map for $d = 7.88$ Å is shown in Fig. 4a for comparison with the constant-height AFM measurement in Fig. 4b. In this measurement, the tip height was ∼0.15 Å greater than in the measurement shown in Fig. 2b, which resulted in slightly reduced contrast. At this height, the qualitative agreement with the calculations is excellent. Comparing Fig. 4a and b, we observe local minima near the position of the oxygen atoms and

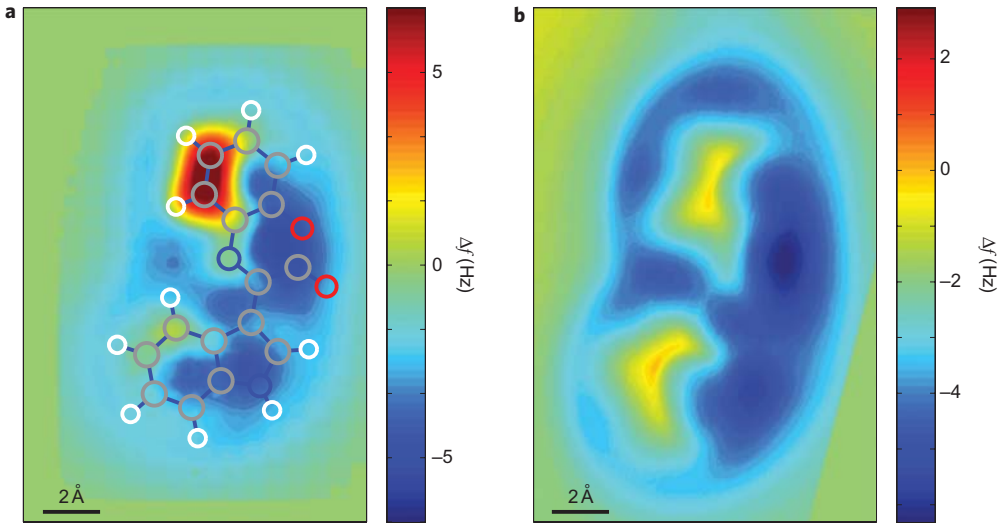

Figure 4 | Comparison of experimental and simulated AFM images. a, Simulated map of the frequency shift, calculated for an intermolecular distance $d = 7.88$ Å. **b**, Constant-height AFM image (imaging parameters $A = 0.5$ Å, $V = 0$ mV). The observed contrast can only be explained by taking into account the non-planar adsorption geometry of the molecule. The good agreement between DFT and experiment validates the structural assignment as **1**.

the NH group, which agree well in their relative intensity and shape. From the calculations, we find that the molecule is mainly bound to the substrate at these sites, which are therefore relaxed toward the surface. Their distances to the topmost NaCl layer are $h(O1) = 2.68$ Å, $h(O2) = 2.52$ Å and $h(N1') = 2.69$ Å, respectively. On the sides opposing the binding sites of the respective bicyclic systems, the distance to the surface becomes maximal ($h(C5) = 3.23$ Å, $h(C4') = 2.97$ Å). This explains the relative maxima observed at the bonds of C5–C6 and C4′–C5′.

Discussion

The calculations demonstrate that by taking into account the non-planar adsorption geometry of the molecule, the observed AFM contrast can be reproduced. Moreover, we confirm that the method is highly sensitive to the out-of-plane arrangement of the atom sites. Our measurements show that the investigated molecules do not necessarily have to be strictly planar. However, in general, atomic resolution can only be obtained by this method on the topmost layer of atoms. For this reason, the method remains restricted to molecules consisting of only one layer of atoms, or possibly two layers if measurements on both faces of the molecule can be combined. Therefore, SPM manipulation of molecules might be used to exhibit different facets of a molecule[26] or molecular subgroups[27] for their AFM investigation.

In contrast to **1**, the DFT calculations for **2** show a more planar adsorption geometry ($h(C5) = 2.89$ Å, $h(C4') = 2.89$ Å), with a slight outward relaxation of the oxygen that is part of the six-membered ring ($h(O2) = 2.92$ Å). This topography disagrees with the AFM measurement, and therefore provides further support for the elimination of **2**.

It is interesting to note that in the constant-current AFM image (Fig. 3b) there is a bright spot between H4′ and N4, and the constant-height image (Fig. 2b) shows bright contrast similar to a bond connecting C4′ and N4. The chemical shift of H4′ in the ^{1}H NMR spectrum (8.70 ppm) suggests that a dipolar interaction is taking place with N4, causing the deshielding. This indicates the imaging of a non-classical hydrogen bond. However, this interpretation remains speculative because the feature of a connecting hydrogen bond was not reproduced in the DFT simulated image, whereas the calculations agree well in the relative contrast of N4 and C4′. Confirmation of the direct visualization of hydrogen bonding as also proposed by STHM[22] would be of tremendous benefit to those studying self-assembly by non-covalent interactions on surfaces[28,29].

In conclusion, from our analysis performed with a combination of spectroscopic techniques, AFM imaging and DFT calculations, we can identify **1** as the only possible molecular structure. Structure **1** is consistent with a proposed biogenesis that derives **1** from tryptophan and the phenazine biogenetic precursor *trans*-2,3-dihydro-3-hydroxyanthranilic acid[30]. We have shown that AFM can assist in the determination of the chemical structure of a molecule by directly imaging it with atomic resolution. Comparison of the measured image and adsorption geometry with DFT calculations confirmed the structural assignment. With the ability to conduct biological assays on microgram quantities of natural products, the challenge is now to elucidate structures of bioactive compounds at this level, and novel approaches such as the one reported here are necessary. AFM offers the advantage of directly visualizing bonds, which is complementary to other techniques used for structure determination, and the ability to work with very small quantities of non-crystalline material. We posit that SPM can be used effectively for the direct assignment of planar molecules or those containing planar substructures.

Methods

Spectroscopic measurements and compound isolation. ^{1}H, ^{13}C and all two-dimensional NMR experiments were performed on a Varian Unity INOVA 400 equipped with an inverse detected probe. Low-resolution ESI-MS data were obtained using a Perseptive Biosystems Mariner LC-MS, and high-resolution ESI-MS data were obtained on a Thermo Orbitrap. HPLC separations were carried out using a Phenomenex reversed-phase column (Jupiter 4μm Proteo 90 Å, 250 × 10 mm^2) and an Agilent 1200 series gradient pump monitored using a DAD G1315B variable-wavelength UV detector. The strain of *Dermacoccus abyssi* was isolated as previously reported[15]. Fermentation and the first stages of isolation were carried out as previously reported[31]. Final purification was achieved by reversed-phase HPLC using a gradient of 0–90% CH_3CN/H_2O over 40 min, yielding compound **1** (13.6 mg), as well as a number of dermacozines, which are reported separately[31].

STM and AFM measurements. As substrate we used a Cu(111) single crystal partly covered with two-monolayer-thick islands of NaCl (thermally evaporated at a sample temperature of 270 K). An amount of the order of 10 μg of the molecular compound was solved in methanol and spread on a silicon wafer, from which the molecules where thermally evaporated onto the sample held at ~10 K. The measurements were performed using a combined homebuilt STM and AFM system based on a qPlus sensor design[18] in ultrahigh vacuum at a temperature of 5 K. The bias voltage was applied to the sample. We used a tuning fork with spring constant $k_0 \approx 1.8 \times 10^3$ N m^{-1}, quality factor $Q \approx 50{,}000$ and resonance frequency $f_0 = 27{,}996$ Hz. The AFM was operated in frequency modulation mode[19], and the

AFM images recorded show the detuning Δf of the resonance frequency. We functionalized the tip apex by deliberately picking up a single CO molecule. A few days are typically needed to prepare sample and tip. The acquisition time for an AFM image of an individual molecule is typically ~15–30 min. Further details about the measurement mode and the tip functionalization have been described previously[9].

DFT calculations. We used the highly optimized plane-wave code CPMD[32] and applied the Perdew–Burke–Ernzerhof exchange correlation functional[33]. *Ab initio* norm-conserving pseudopotentials[34] with a plane-wave cut-off energy of 100 Ry were used. The size of the slab considered was 17 Å × 17 Å, and a four-layer-thick NaCl substrate was taken into account. Our calculations yielded adsorption energies of 2.06 and 2.20 eV for **1** and **2**, respectively. For **2** the total energy decreased by ~1.2 eV when the structure was relaxed, starting from the experimentally determined adsorption position. As we observed no effect in the interaction energy when removing the NaCl layers, we omitted the NaCl substrate for calculating the image shown in Fig. 4a.

Received 15 April 2010; accepted 18 June 2010; published online 1 August 2010

References

1. Binnig, G. & Rohrer, H. Scanning tunneling microscopy. In *Trends in Physics 1984 Proc. 6th Gen. Conf. Europ. Phys. Soc.* Vol. 1 (eds Janta, J. & Pantoflíček, J.) 38–46 (EPS, 1984).
2. Driscoll, R. J., Youngquist, M. G. & Baldeschwieler, J. D. Atomic-scale imaging of DNA using scanning tunnelling microscopy. *Nature* **346,** 294–296 (1991).
3. Heckl, W. *et al.* Two-dimensional ordering of the DNA base guanine observed by scanning tunneling microscopy. *Proc. Natl Acad. Sci. USA* **88,** 8003–8005 (1991).
4. Otero, R. *et al.* Guanine quartet networks stabilized by cooperative hydrogen bonds. *Angew. Chem. Int. Ed.* **44,** 2270–2275 (2005).
5. Shapir, E. *et al.* Electronic structure of single DNA molecules resolved by transverse scanning tunnelling spectroscopy. *Nature Mater.* **7,** 68–74 (2008).
6. Tanaka, H. & Kawai, T. Partial sequencing of a single DNA molecule with a scanning tunnelling microscope. *Nature Nanotech.* **4,** 518–522 (2009).
7. Baker, A. A., Helbert, W., Sugiyama, J. & Miles, M. J. New insight into cellulose structure by atomic force microscopy shows the I_α crystal phase at near-atomic resolution. *Biophys. J.* **79,** 1139–1145 (2000).
8. Scheuring, S., Reiss-Husson, F., Engel, A., Rigaud, J. L. & Ranck, J. L. High-resolution AFM topographs of *Rubrivivax gelatinosus* light-harvesting complex LH2. *EMBO J.* **20,** 3029–3035 (2001).
9. Gross, L., Mohn, F., Moll, N., Liljeroth, P. & Meyer, G. The chemical structure of a molecule resolved by atomic force microscopy. *Science* **325,** 1110–1114 (2009).
10. Crews, P., Rodríguez, J. & Jaspars, M. *Organic Structure Analysis* (Oxford Univ. Press, 2010).
11. Blunt, J., Copp, B., Munro, M., Northcote, P. & Prinsep, M. Marine natural products. *Nat. Prod. Rep.* **27,** 165–237 (2010).
12. Amagata, T. In *Comprehensive Natural Products II Chemistry and Biology* (eds Mander, L. & Lui, H.-W.) (Elsevier, 2010).
13. Nicolaou, K. C. & Snyder, S. A. Chasing molecules that were never there: misassigned natural products and the role of chemical synthesis in modern structure elucidation. *Angew. Chem. Int. Ed.* **44,** 1012–1044 (2005).
14. Maier, M. E. Structural revisions of natural products by total synthesis. *Nat. Prod. Rep.* **26,** 1105–1124 (2009).
15. Pathom-Aree, W. *et al.* Diversity of *Actinomycetes* isolated from Challenger Deep sediment (10,898 m) from the Mariana Trench. *Extremophiles* **10,** 181–189 (2006).
16. Wu, P.-L., Hsu, Y.-L. & Jao, C.-W. Indole alkaloids from *Cephalanceropsis gracilis*. *J. Nat. Prod.* **69,** 1467–1470 (2006).
17. Mason, J., Bergman, J. & Janosik, T. Synthetic studies of Cephalandole alkaloids and the revised structure of Cephalandole A. *J. Nat. Prod.* **71,** 1447–1450 (2008).
18. Giessibl, F. J. High-speed force sensor for force microscopy and profilometry utilizing a quartz tuning fork. *Appl. Phys. Lett.* **73,** 3956–3958 (1998); Erratum: *Appl. Phys. Lett.* **74,** 4070 (1999).
19. Albrecht, T., Grütter, P., Horne, D. & Rugar, D. Frequency modulation detection using high-Q cantilevers for enhanced force microscope sensitivity. *J. Appl. Phys.* **69,** 668–673 (1991).
20. Giessibl, F. J. Advances in atomic force microscopy. *Rev. Mod. Phys.* **75,** 949–983 (2003).
21. Temirov, R., Soubatch, S., Neucheva, O., Lassise, A. & Tautz, F. A novel method achieving ultra-high geometrical resolution in scanning tunnelling microscopy. *New J. Phys.* **10,** 053012 (2008).
22. Weiss, C. *et al.* Resolving chemical structures in scanning tunnelling microscopy. Preprint at http://arxiv.org/abs/0910.5825v1 (2010).
23. Sugimoto, Y. *et al.* Chemical identification of individual surface atoms by atomic force microscopy. *Nature* **446,** 64–67 (2007).
24. Hohenberg, P. & Kohn, W. Inhomogeneous electron gas. *Phys. Rev.* **136,** B864–B871 (1964).
25. Kohn, W. & Sham, L. J. Self-consistent equations including exchange and correlation effects. *Phys. Rev.* **140,** A1133–A1138 (1965).
26. Keeling, D. L., Humphry, M. J., Fawcett, R. H. J., Beton, P. H., Hobbs, C. & Kantorovich, L. Bond breaking coupled with translation in rolling of covalently bound molecules. *Phys. Rev. Lett.* **94,** 146104 (2005).
27. Moresco, F., Meyer, G., Rieder, K.-H., Tang, H., Gourdon, A. & Joachim, C. Conformational changes of single molecules induced by scanning tunneling microscopy manipulation: a route to molecular switching. *Phys. Rev. Lett.* **86,** 672–675 (2001).
28. Theobald, J. A. *et al.* Controlling molecular deposition and layer structure with supramolecular surface assemblies. *Nature* **424,** 1029–1031 (2003).
29. Champness, N. R. Molecular imaging: the tip of what can be seen. *Nature Chem.* **1,** 597–598 (2009).
30. Mavrodi, D., Blankenfeldt, W. & Thomashow, L. Phenazine compounds in fluorescent *Pseudomonas* Spp. biosynthesis and regulation. *Annu. Rev. Phytopathol.* **44,** 417–445 (2006).
31. Abdel-Mageed, W. *et al.* Dermacozines, a new phenazine family from deep-sea dermacocci isolated from a Mariana Trench sediment. *Org. Biomol. Chem.* doi: 10.1039/C001445A (2010).
32. CMPD, CPMD Consortium, Copyright IBM Corp. 1990–2008, Copyright MPI für Festkörperforschung Stuttgart 1997–2001.
33. Perdew, J. P., Burke, K. & Ernzerhof, M. Generalized gradient approximation made simple. *Phys. Rev. Lett.* **77,** 3865–3868 (1996).
34. Hamann, D. R. Generalized norm-conserving pseudopotentials. *Phys. Rev. B* **40,** 2980–2987 (1989).

Acknowledgements

The authors thank K. Horikoshi for providing the Mariana Trench sediment, and A. Bull and M. Goodfellow for providing the *Dermacoccus abyssi* strain. Thanks also go to A. Curioni and R. Allenspach for discussions and comments. The research leading to these results has received funding from the European Community's projects HERODOT (grant agreement no. 214954) and ARTIST (grant agreement no. 243421) and the Swiss National Center of Competence in Research (NCCR) 'Nanoscale Science'. W.M.A.M. received a PhD scholarship from the Egyptian government, and Aberdeen University provided instrument access. M.J. is the recipient of a BBSRC Research Development fellowship. The EPSRC National Mass Spectrometry Service provided the MS data. M.J. acknowledges S. Jaspars for bringing the work of the IBM team to his attention.

Author contributions

L.G., F.M. and G.M. performed the STM/AFM experiments. N.M. carried out the DFT calculations. R.E., W.M.A.M. and M.J. performed the NMR characterization and mass spectrometry. All authors contributed to the analysis of the data and the writing of the manuscript.

Additional information

The authors declare no competing financial interests. Supplementary information and chemical compound information accompany this paper at www.nature.com/naturechemistry. Reprints and permission information is available online at http://npg.nature.com/reprintsandpermissions/. Correspondence and requests for materials should be addressed to L.G.